Learning Human-Blockage Direction Prediction from Indoor mmWave Radio Measurements

Praneeth Susarla*, Markku Jokinen†, Nuutti Tervo†, Marko E. Leinonen†,
Miguel Bordallo Lopez*, Markku Juntti†, and Olli Sílven*
*Center for Machine Vision and Signal Analysis (CMVS), University of Oulu, Oulu FI-90014, Finland
†Center for Wireless Communications (CWC), University of Oulu, Oulu FI-90014, Finland
Email: { praneeth.susarla, markku.jokinen, nuutti.tervo, marko.e.leinonen, miguel.bordallo, markku.juntti, olli.silven}@oulu.fi

***Abstract*—Millimeter wave (mmWave) beamforming is a vital component of the fifth generation (5G) new radio (NR) and beyond wireless communication systems. The usage of mmWave narrow beams encounters frequent signal attenuation due to random human blockages in indoor environments. Human blockage predictions can jointly improve the signal quality as well as passively sense human activities during mmWave communication. Human sensing using wireless fidelity (WiFi) systems has earlier been studied using receiver signal strength indicator (RSSI) signal level fluctuations based on distance measurements. Other conventional approaches using cameras, lidars, radars, etc. require additional hardware deployments. Current device-free WiFi sensing approaches use vendor-specific channel state information to obtain fine-grained human blockage predictions. Our novelty in this work is to obtain fine-grained human blockage direction predictions in mmWave spectrum, using a time series of RSSI measurements and build fingerprints. We perform experiments to construct a Human Millimetre-wave Radio Blockage Detection (HuMRaBD) dataset and observe human influence in different radio beam directions during each radio initial access procedure. We design a multi layer perceptron (MLP) framework to analyze the HuMRaBD dataset over coarse-grained and fine-grained mmWave blockage directions from static and dynamic human movements. The results show that our trained MLP-trained models can simultaneously sense multiple indoor human radio-blockage directions at an average F1 score of 0.84 and area under curve (AUC) score of 0.95 during mmWave communication.**

***Index Terms*—5G and beyond, 6G, joint communication and sensing, mmWave, multi layer perceptron**

I. Introduction

Millimeter wave (mmWave) beamforming is an integral component of fifth generation (5G) new radio (NR) and beyond communication systems due to its considerable increase in data rate owing to the wider bandwidth. However, the usage of narrow beams at mmWave frequencies poses greater signal attenuation challenges due to blockages, channel variation, atmospheric attenuation etc. [1]. Especially, the random blockages from humans at multiple instants can significantly degrade the link quality in mmWave and beyond communications [2]. To minimize such adverse effects, it is essential to detect human blockages either to allow proactive handover procedures with LOS availability between the radios or to prevent the communication in blockage direction.

Wireless fidelity (WiFi) sensing relying on received signal strength indicator (RSSI) fluctuations has been extensively studied using IEEE802.11n systems for localization, tracking and recognition of human activities [3], [4]. However, these RSSI fluctuations relied only on distance measurements and hence considered only for coarse-grained human activity detection. Channel state information (CSI)-based WiFi sensing approaches provide a more detailed information and has also been studied for human detection and recognition tasks [5]–[7]. However, the CSI-based information although included since IEEE802.11n, is vendor specific and hence difficult to use off-the-shelf WiFi devices to perform fine-grained human blockage predictions [7].

Recent works perform human blockage prediction from heterogenous modalities such as camera, lidar and radars etc. [8]–[10] for mmWave communications. Human blockage prediction using these modalities can be accurate as they provide a wider view of the environment thereby improving beam alignment accuracy. However, this requires the deployment of additional hardware, and sensor synchronization at different sampling rates alongside the wireless links in the indoor environments. Model-based human blockage detection using radio signals has also been proposed in the literature [11]–[13]. In [11], authors survey the comparison of different human blockage models using distance-dependent human shadowing until 30 GHz based on diffraction measurements. The authors in [12], extend the survey by providing more insights into body-orientation, antenna height, material etc. dependence on three-dimensional (3D) human-blockage models as they cause temporal variation to the radio channel. However, these mathematical models are complex and specific to the chosen indoor environmental conditions.

In this paper, we design a model-free and a device-free human-blockage prediction using emerging machine learning (ML) intelligence and mmWave radio measurements. The radio frequency (RF) signal characteristics and information during mmWave communication is influenced by the presence of human body objects and their directional movements in the environment causing phenomena like reflections, diffraction, scattering etc. Hence, we capture the RSSI information at the receiver to observe such influential changes in the form of radio fingerprints and predict radio blockage directions using ML tools like multi layer perceptron (MLP). We conduct our radio-blockage prediction experiments with a universal software radio peripheral (USRP) up-converted mmWave setup operating at 28 GHz frequency [14]. Our human blockage

direction prediction results from mmWave radio measurements achieve an average F1 score of 0.84 and area under curve (AUC) score of 0.95.

The rest of the paper is organized as follows. Section II describes the radio communication system and its hardware implementation to capture the mmWave radio measurements. Section III discuss in detail the dataset design and collection procedure using RF dataset. The Section IV presents the comparison of human-blockage prediction against different dataset classes. Section V summarizes the conclusion and future work.

II. Signal Processing System and Implementation

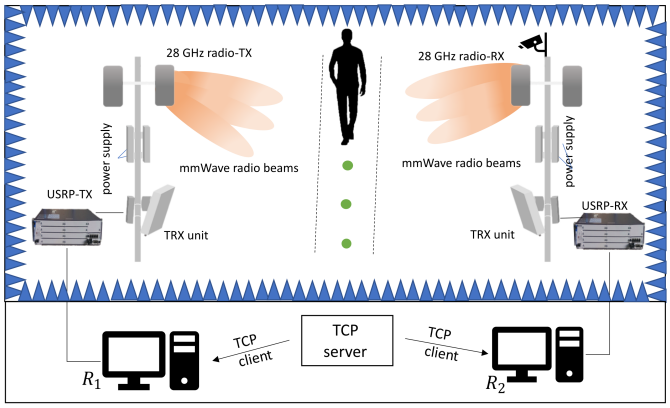

Figure 1: mmWave radio with USRP communication system in an indoor laboratory environment.

A. Experimental Setup

We consider an indoor anechoic environment consisting of mmWave radios, baseband communication units and a camera as shown in Figure 1. The mmWave radio equipment consists of TX and RX radio units located at a 4m distance from one another at two corners of the room. Both RX and TX units are each equipped with USRP-N310 units[1] to support baseband communication. A microsoft lifecam camera[2] is mounted on RX to capture the human moving patterns and location in the indoor environment with respect to the radio receiver. The captured camera information extracts the ground truth labels for radio-based human blockage prediction. A set of green markers representing different radio blockage or refraction directions with respect to RX are also arranged between the two radio transceivers. These markers are used to capture the human radio blockage directions from the camera, with respect to RX. In this work, we assume markers are placed along a straight line and the radio-blockage directions are only predicted for humans moving along the line following markers as shown in Figure 1. However, the proposed method is not limited to this assumption and can be extended to different indoor human movements in future. The USRP baseband and mmWave radio signals are monitored and controlled by computing sources separately at TX and RX, respectively.

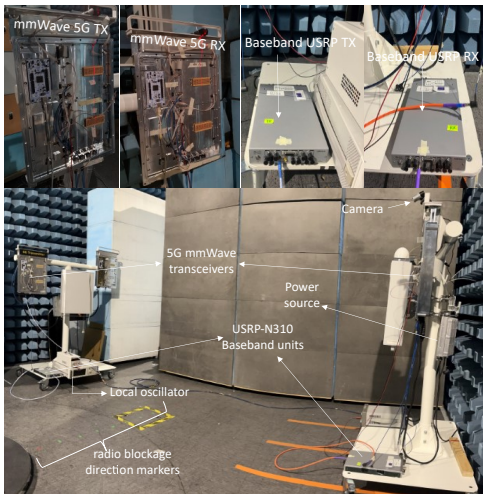

Figure 2: Experimental setup

B. Radio Communication System

We consider a 5G NR radio communication system with a backhaul unit as shown in Figure 1. The characterization and usage of the backhaul radio transceiver is presented in [14]. The radio front-end units of the transceiver operate at 28 GHz mmWave frequency with an effective isotropic radiation power (EIRP) of 45 dBm. Both the TX and RX units are equipped with 64-element mmWave phased array [15] and are arranged in a 16×4 formation. The array is further divided into 16 unit cells each having 4 elements configured as 2×2 smaller subarray. Each of the unit cell path is equipped with a power amplifier (PA)/ low noise amplifier (LNA) and the time division duplex (TDD) switch. To facilitate mmWave beamforming in the hardware, each of the 16 paths also possess an individual digitally controlled 5-bit phase shifter. The software defined radio (SDR) USRP-N310 acts as the baseband units at both ends of the transceiver. The USRP-TX transmits the baseband signal using orthogonal frequency division multiple access (OFDM) with 64 fast fourier transform (FFT) size, 48 subcarriers and QPSK modulation at 4 GHz intermediate frequency (IF) and 1 MHz bandwidth. The 4 GHz IF signal is then upconverted to 28 GHz mmWave RF during over-the-air (OTA) communication signal transmission. We note that the 1 MHz bandwidth (for mmWave frequencies) is selected due to the trade-off between sampling rate and measurement speed of USRPs to support our experiments. Similarly at RX, mmWave RF signal is obtained and then down converted to IF signals to receive the baseband data. Figure 2 display the USRPs, mmWave transceivers and the experimental setup used for the 5G NR OTA measurements. The interfaces between the baseband and transceiver radio units are described in [16]. The USRP baseband data is monitored using GNU radio-python and RF beam steering is controlled using MATLAB interfaces by the computing resources at TX and RX, respectively.

[1]https://www.ettus.com/wp-content/uploads/2019/01/USRP_N310_Datasheet_v3.pdf

[2]https://www.microsoft.com/en/accessories/products/webcams/lifecam-studio?activetab=pivot:overviewtab

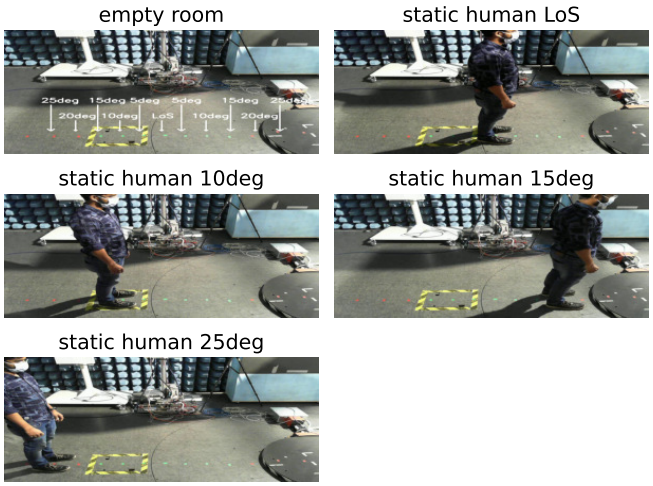

Figure 3: Images of human blocking different radial directions in the laboratory environment under HuMRaBD dataset.

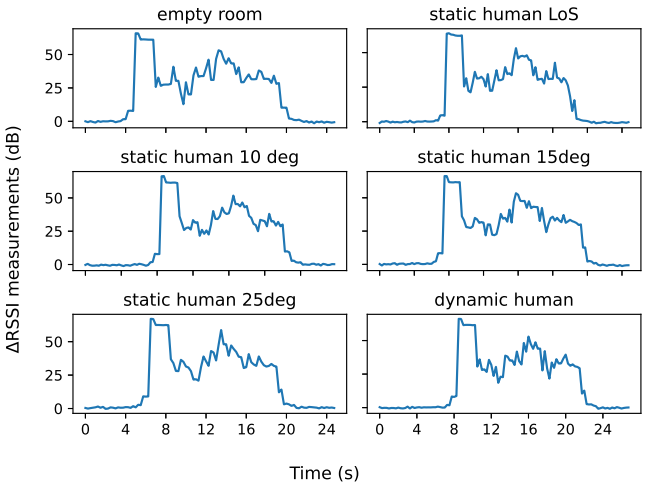

Figure 4: Change in RSSI measurements for multiple human radio-blockage directions in the HuMRaBD dataset.

C. Communication Radio-Blockage Measurement Setup

Wireless dynamic signal's characteristics and information during communication is influenced by the human random movements inside the environment. By observing the dynamic changes in radio signal characteristics such as received signal level, received signal data rate, received signal quality etc. over time, human radio blockages and their activities can be estimated. The 5G NR beamforming protocol starts with a four-stage synchronisation signal (SS) block-based initial access (IA) followed by different random beam selection procedures such as exhaustive, hierarchical and other fast beam alignment algorithms [17]. Under this protocol, each SS burst followed by beam selection appear periodically after 20 ms [18]. By observing the dynamic changes in signal characteristics from the beam-selection process in multiples of these periodic bursts during communication, human radio blockage directions can be estimated over time. In this work, we employ the traditional exhaustive beam-search methodology to scan human blockage or refraction directions in mmWave RF environment and capture the baseband RSSI characteristics at RX. We note that the MATLAB interface is used to synchronize and also select beam steering directions of TX and RX using computing resources R_1 and R_2, respectively. We also simultaneously initiate and cease the measurement setup using GNU radio-python and MATLAB interfaces, to synchronize the captured information from both camera and USRP baseband units.

Table I: Human mmWave radio-blockage direction-based activities

Class activity	Label
No human/empty room	1
Static human at LoS	2
Static human at 10°	3
Static human at 15°	4
Static human at 25°	5
Dynamic human	6

III. Dataset Collection and Learning Formulation

In this section, we first describe the radio-blockage data collection procedure using the measurement setup illustrated in section II. Secondly, we formulate the learning-based human radio blockage detection using the collected communication data.

A. Human Radio-Blockage Dataset

We construct a Human Millimeter wave Radio Blockage Detection (HuMRaBD) dataset using the measurement setup (described in section II) in an anechoic indoor environment as shown in Figure 1. The dataset consists of 17 subjects with each subject performing a set of human radio-blockage activities defined as dataset classes between the RX and TX. The antennas in 5G mmWave system are observed to operate reliably in the RF beam angular region $[-30°.....+30°]$ [16]. Hence we place the green markers in our indoor environment setup (as shown in Figure 1), within the aforementioned region at a $5°$ angular resolution between them. For the HuMRaBD dataset, we define 6 radio-blockage classes with labels as shown in Table I. Each subject class activity follow a protocol to collect the camera and radio data as given below:

1) Camera and mmWave communication system are turned on simulatenously
2) RF transceivers are backhaul synchronized using R_1 and R_2 using TCP server
3) TX and RX radio units perform exhaustive beam search following mmWave radio procedure at 28 GHz
4) During each beam search, RF signals at RX are demodulated to a baseband signal at USRP-RX and stored as the radio data.
5) Human activity video-feed is captured and stored as the camera data
6) At the end of mmWave radio procedure, both the radio and camera systems are turned off respectively.

The collected radio signals in the dataset consist of RSSI information to analyse human radio-blockage directions in the indoor environment. Inside the anechoic communication environment, RSSI represents a sum of signal energy from multiple paths which include a dominant line-of-sight (LoS) path between TX and the RX, and multiple minor reflective paths caused by surrounding objects and humans. Blocking the dominant communication path contributes to a significant change in radio signal information. Thus, we argue that only RSSI information maybe sufficient to observe and capture the change in radio signal information for every IA procedure. We assume noise floor level as 0 dB and measure RSSI of the received signals in decibels (dB):

$$\text{RSSI} = 10\log_{10}\|V\|^2, \tag{1}$$

where V and $\|.\|^2$ denote the received signal and L_2 norm, respectively.

Figure 3 shows the example screenshots of different static human positions from the HuMRaBD video dataset. Also, the emptyroom screenshot display the angular direction annotations of various markers measured with respect to RX. During each class activity, the protocol performs an exhaustive beam-search in 28 GHz spectrum by sweeping the beams from 25° from left (-25° in angular region) to 25° at right ($+25^\circ$ in angular region) inside the screenshot, at both TX and RX. For the dynamic human activity, subject is allowed to walk randomly along the straight line perpendicular to TX-RX units between -25° to $+25^\circ$ markers. For this work, we only assume dynamic movements and static positions along the straightly arranged markers. However, the proposed approach is not limited to this assumption and can be extended to other indoor movements as well in future.

Figure 4 displays the change in RSSI measurements captured over time for different corresponding class activities (from Figure 3) of a subject in HuMRaBD dataset. Firstly, the captured video length RSSI measurements are sampled at a specific sampling rate and then a change in RSSI level among the consecutive samples is acquired. In this work, we heuristically obtain the sample rate based on the captured video length and the USRP measurements. As shown in these subplots, different RSSI signatures can be observed with change in magnitudes and shifted patterns (in dB with respect to noise floor level) for different class activities. The shifted pattern in ΔRSSI is mainly due to different static angular positions.

For the dynamic human activity, a significant change can be observed in fingerprints during random walking movements. However, we note the RSSI patterns for dynamic human activity is influenced by human walking speed as well. Also, the common initial peak in fingerprints is due to the change in RSSI level (from 0 reference) at the start of synchronization. Thus, the direction patterns from mmWave spectrum are converted into a time series information of video length by using baseband RSSI measurements. The FFT over a time series data generally represents the information similar to Doppler spectrum of channel. In this work, we perform FFT over the real-valued ΔRSSI information and utilize them as the RSSI fingerprint to classify different radio-blockage direction-based activities.

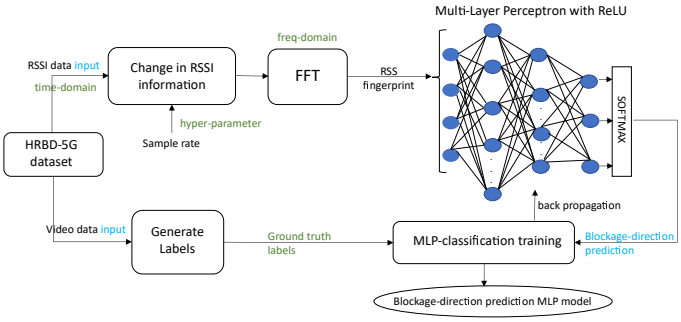

Figure 5: Learning framework for mmWave radio-blockage prediction

B. Learning Framework for Human radio-blockage prediction

The HuMRaBD dataset capture and collects the RSSI data for each blockage activity time during each IA procedure of RF communication. However, the obtained raw data is less intuitive to obtain the human blockage direction information. Hence, we employ ML to model a classification problem on the collected data and predict the blockage directions for each subject activity. Firstly, we pre-process the raw radio signals by observing the consecutive change in RSSI information along the collected time-domain samples. Such information is converted into frequency domain and serves as the radio fingerprint for the corresponding blockage activity.

We design a MLP to model this ML classification problem. In this work, the MLP architecture contains two fully connected layers with 128 and 32 neurons, respectively along with rectifier linear units (ReLU) activation. The captured RSSI fingerprint serves as input into the network while the output layer contains neurons equal number of dataset classes. More details on the learning framework is illustrated in Figure 5.

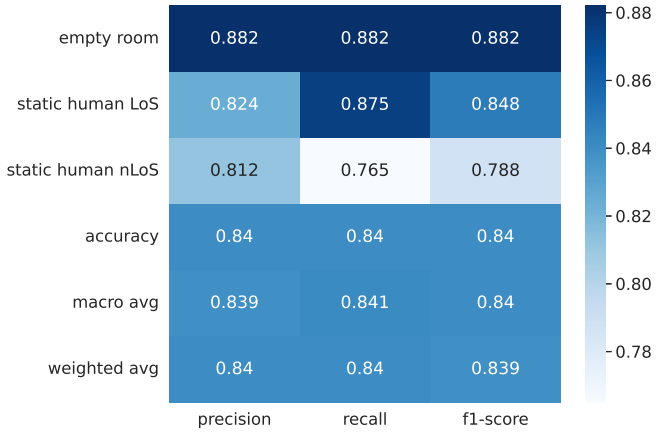

Figure 6: mmWave radio-blockage MLP prediction for no human, human at LoS, human at nLoS classes.

IV. Experiment Results

As described in section II and section III-C, we implement a MLP model to predict the radio blockage direction of human on a 5G HuMRaBD dataset. In this section, we evaluate the performance of MLP model over different sets of class activities. As the dataset is relatively small, we perform the MLP model training for all simulations in a cross-validation manner.

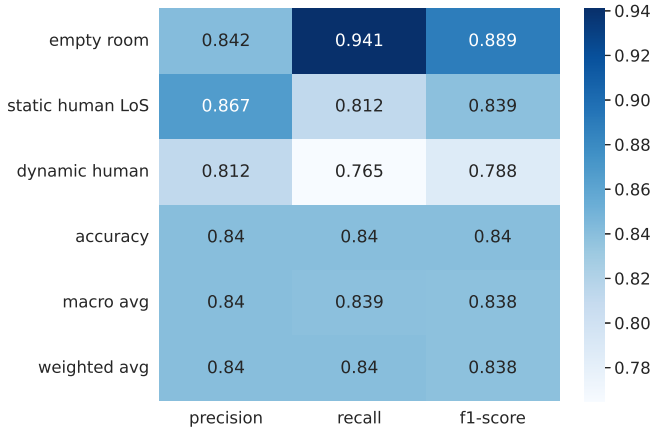

Figure 7: mmWave radio-blockage MLP prediction for no human, static human LoS, dynamic human.

A. Coarse-grained Human Blockage-direction Classification

In this experiment, we train the MLP architecture to predict coarsely-grained mmWave blockage direction classes such as empty room/no human, static human blocking LoS direction, static human blocking non-line-of-sight (nLoS) direction, and dynamic human. To prevent any class imbalance during training, we consider the nLoS direction data only from one of the nLoS class samples from HuMRaBD dataset (say, label 3 radio samples in Table I). F1 score is a ML metric that combines classification precision and recall performance and measure the model's accuracy [19]. We evaluate the trained MLP model performance by comparing the blockage direction predictions against the ground truth in the form of a classification report using precision, recall and F1 score metrics as shown in Figure 6 and Figure 7. Firstly, we train a 3 class MLP model to classify empty room, static human at LoS and static human at nLoS labels. We observe that the MLP model accurately predicts the LoS and nLoS blockage directions from a empty room at an average F1 score of 0.84. Secondly, we model the same MLP architecture over different set of 3 classes such as empty room, static human and dynamic human labels. We observe that the retrained MLP model with same architecture accurately predicts the human absence from static and dynamic human activities in the indoor environment at a similar average F1 score of 0.84. Thus, the fingerprints obtained from mmWave radio signals can help to simultaneously sense different coarse-grained blockage direction classes during communication.

B. Fine-grained Human Blockage-direction Classification

In this experiment, we consider the MLP multi-class classification with fine-grained nLoS mmWave blockage directions by considering all static human labels from Table I. We evaluate the trained MLP model performance for all 5 classes (label 1 to label 5 in Table I) by plotting a receiver operating characteristic (ROC) curve per blockage direction label as shown in Figure 8. The ROC curves use the probabilistic predictions from the MLP classifier and predicts the accuracy for each blockage direction label using true positive rate (TPR) and false positive rate (FPR) metrics. We use AUC scores to measure the ROC curve for each label and compare the MLP overall performance to a random classifier [19]. We observe that the MLP model successfully predicts the LoS and different nLoS blockage directions even at narrow angular resolution in the indoor environment. Moreover, the ROC plots for nLoS directions are observed to perform slightly better compared to that of LoS direction prediction curve. This could be due to the influence of (5°) narrow beam angular resolution, different body dimensions and LoS static position errors of subjects from the collected dataset. However, the MLP model classifies the narrow beam blockage directions with an average AUC score of 0.95 compared to a random classifier with 0.5 AUC. Thus, the fingerprints obtained from mmWave radio signals are reliable to simultaneously sense narrow angular blockage directions during communication.

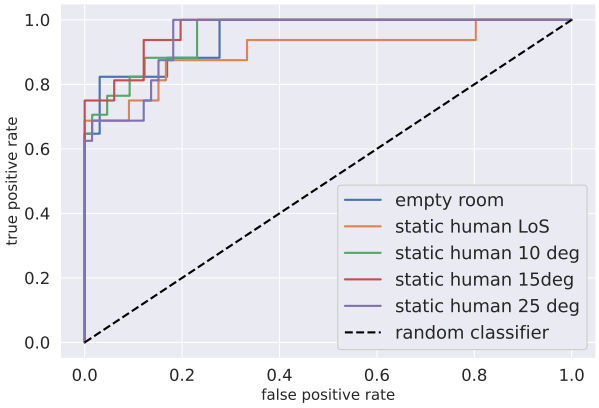

Figure 8: ROC curves for MLP-based fine-grained blockage direction predictions in HuMRaBD dataset.

C. Blockage-direction Classification for static and dynamic human movements

In this experiment, we consider the radio blockage data from both static as well as dynamic human movements under the MLP training. We evaluate the trained MLP model performance by comparing the blockage direction predictions against the actual values for all 6 classes (labels 1 to label 6 in Table I) as shown in Figure 9. We observe that the MLP model predicts the human movements and also differentiates accurately from an empty room with a reliable average AUC score of 0.94

compared to the random classifier's 0.5 AUC. We also observe here a slight decrease in an average F1 score (0.75) compared to coarse-grained MLP-based blockage direction prediction models. The dynamic humans walking at different speeds may induce multiple radial direction blockages inherently. As a result, a decrease in individual F1 scores among the static blockage direction labels is observed due to the inclusion of dynamic human fingerprints (in the MLP training) and hence, impacting the average F1 score prediction accuracy. However, the overall MLP performance for this classification achieves an average AUC score of 0.94 similar to fine-grained blockage prediction. Thus, the fingerprints obtained from mmWave radio signals are reliable to simultaneously sense narrow angular blockage directions, and static-dynamic human movements during communication.

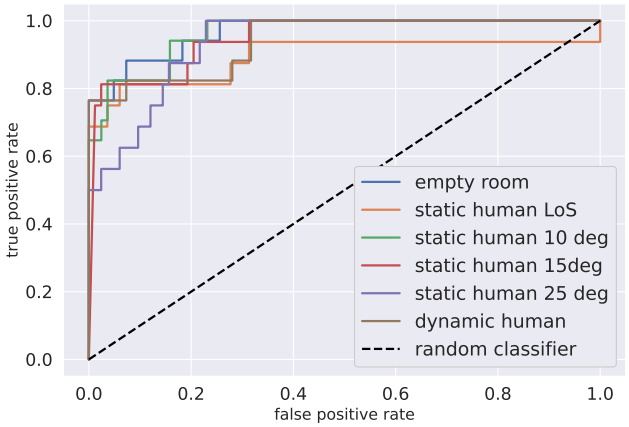

Figure 9: mmWave radio-blockage prediction using MLP for no human, human at LoS, no human at nLoS, human walking classes.

V. Conclusion and Future Work

In this paper, we proposed a learning framework for human-blockage prediction from indoor mmWave communication radio measurements. We design a framework to extract human-blockage direction information from the mmWave signals observed during each radio IA communication procedure. We perform experiments and construct a HuMRaBD dataset containing both video and radio data by emulating indoor human blockages in a controlled indoor anechoic environment. We also model the HuMRaBD dataset using MLP architecture to perform coarse-grained and fine-grained multi-class blockage direction classification from communication radio measurements. Our results have shown that the MLP-based mmWave radio fingerprint approach can simultaneously sense multiple radio-blockage directions during each communication IA procedure at an average F1 score of 0.84 and AUC score of 0.95. Having shown some promising results, we will extend the MLP-based framework with data collection from multiple indoor environments, increased subjects, increased blockage directions, back-scattering signals etc. as future works.

Acknowledgements

This work was supported in part by the Academy of Finland projects 6Genesis Flagship (grant number 346208) and Jenny-Antti Wihuri Foundation (grant number 220380).

References

[1] B. Ji, Y. Han, S. Liu, F. Tao, G. Zhang, Z. Fu, and C. Li, "Several key technologies for 6g: challenges and opportunities," *IEEE Communications Standards Magazine*, vol. 5, no. 2, pp. 44–51, 2021.

[2] G. R. MacCartney, T. S. Rappaport, and S. Rangan, "Rapid fading due to human blockage in pedestrian crowds at 5g millimeter-wave frequencies," in *GLOBECOM 2017 - 2017 IEEE Global Communications Conference*, 2017, pp. 1–7.

[3] K. El-Kafrawy, M. Youssef, A. El-Keyi, and A. Naguib, "Propagation modeling for accurate indoor wlan rss-based localization," in *2010 IEEE 72nd Vehicular Technology Conference-Fall*. IEEE, 2010, pp. 1–5.

[4] H. Abdelnasser, M. Youssef, and K. A. Harras, "Wigest: A ubiquitous wifi-based gesture recognition system," in *2015 IEEE Conference on Computer Communications (INFOCOM)*, 2015, pp. 1472–1480.

[5] R. Zhou, X. Lu, P. Zhao, and J. Chen, "Device-free presence detection and localization with svm and csi fingerprinting," *IEEE Sensors Journal*, vol. 17, no. 23, pp. 7990–7999, 2017.

[6] F. Zhang, C. Chen, B. Wang, and K. R. Liu, "Wispeed: A statistical electromagnetic approach for device-free indoor speed estimation," *IEEE Internet of Things Journal*, vol. 5, no. 3, pp. 2163–2177, 2018.

[7] Y. Ma, G. Zhou, and S. Wang, "Wifi sensing with channel state information: A survey," *ACM Computing Surveys (CSUR)*, vol. 52, no. 3, pp. 1–36, 2019.

[8] D. Marasinghe, N. Rajatheva, and M. Latva-aho, "Lidar aided human blockage prediction for 6g," in *2021 IEEE Globecom Workshops (GC Wkshps)*. IEEE, 2021, pp. 1–6.

[9] M. Alrabeiah, A. Hredzak, and A. Alkhateeb, "Millimeter wave base stations with cameras: Vision-aided beam and blockage prediction," in *2020 IEEE 91st vehicular technology conference (VTC2020-Spring)*. IEEE, 2020, pp. 1–5.

[10] S. Z. Gurbuz and M. G. Amin, "Radar-based human-motion recognition with deep learning: Promising applications for indoor monitoring," *IEEE Signal Processing Magazine*, vol. 36, no. 4, pp. 16–28, 2019.

[11] W. Qi, J. Huang, J. Sun, Y. Tan, C.-X. Wang, and X. Ge, "Measurements and modeling of human blockage effects for multiple millimeter wave bands," in *2017 13th International Wireless Communications and Mobile Computing Conference (IWCMC)*. IEEE, 2017, pp. 1604–1609.

[12] U. T. Virk and K. Haneda, "Modeling human blockage at 5g millimeter-wave frequencies," *IEEE Transactions on Antennas and Propagation*, vol. 68, no. 3, pp. 2256–2266, 2020.

[13] A. Alyosef, S. Rizou, Z. D. Zaharis, P. I. Lazaridis, A. M. Nor, O. Fratu, S. Halunga, T. V. Yioultsis, and N. V. Kantartzis, "A survey on the effects of human blockage on the performance of mm wave communication systems," in *2022 IEEE International Black Sea Conference on Communications and Networking (BlackSeaCom)*, 2022, pp. 249–253.

[14] M. E. Leinonen, M. Jokinen, N. Tervo, O. Kursu, and A. Pärssinen, "System evm characterization and coverage area estimation of 5g directive mmw links," *IEEE Transactions on Microwave Theory and Techniques*, vol. 67, no. 12, pp. 5282–5295, 2019.

[15] M. Sonkki, S. Myllymäki, N. Tervo, M. E. Leinonen, M. Sobocinski, G. Destino, and A. Pärssinen, "Linearly polarized 64-element antenna array for mm-wave mobile backhaul application," in *12th European Conference on Antennas and Propagation (EuCAP 2018)*, 2018, pp. 1–5.

[16] P. Susarla, J. Saloranta, G. Destino, O. Kursu, M. Sonkki, M. E. Leinonen, and A. Pärssinen, "Smart-rf for mmwave mimo beamforming," in *2018 IEEE 29th Annual International Symposium on Personal, Indoor and Mobile Radio Communications (PIMRC)*, 2018, pp. 1–6.

[17] P. Susarla, B. Gouda, Y. Deng, M. Juntti, O. Silven, and A. Tölli, "Learning-based beam alignment for uplink mmwave uavs," *IEEE Transactions on Wireless Communications*, pp. 1–1, 2022.

[18] E. Dahlman, S. Parkvall, and J. Skold, *5G NR: The next generation wireless access technology*. Academic Press, 2020.

[19] A. Géron, *Hands-on machine learning with Scikit-Learn, Keras, and TensorFlow*. " O'Reilly Media, Inc.", 2022.